 CMES, vol.4, no.3&4, pp.397-403, 2003

A Method for Estimating Relative Bone Loads from CT Data with Application to the Radius and the Ulna

K.J. Fischer[1,2], J.A. Bastidas[3], H.J. Pfaeffle[2] and J.D. Towers[2]

Abstract: The two bones of the forearm, the radius and the ulna, have been shown to bear different proportions of the overall forearm load at the wrist and the elbow. This biomechanical data suggests load transfer between the bones occurs through the soft tissues of the forearm. Load transfer from radius to ulna through passive soft tissues such as the interosseous ligament (IOL) has been experimentally measured. Ex vivo studies of the forearm, however, cannot account for the effect of internal loads generated by the muscles and, in some cases, external forces acting directly on the forearm bones. The objective of this study was to estimate the relative loads in the radius and ulna for a range of proximal-distal levels in the forearm, accounting for all in vivo mechanical stimuli. This objective was accomplished using a computational technique based on bone remodeling theory and computed tomography (CT) data of the bones. The results indicate a monotonic exchange of load from the radius, which was found to carry the majority of the load distally, to the ulna, which was found to carry most of the load proximally. Because the load transfer was distributed along the forearm, instead of concentrated in the region of the IOL, it appears that muscle forces may play an important role in load transfer and the overall loading of the forearm bones.

keyword: Forearm, radioulnar, biomechanics, modeling.

1 Introduction

Load transfer at the wrist and the elbow and radioulnar load sharing has long been a topic of interest in the upper extremity. Palmer and Werner [Palmer and Werner (1984)] published classic experiments on the loads in the radius and ulna. Their data indicates that about 60-80% of the load at the wrist is transferred from the carpal bones to the (distal) radius. Rabinowitz, Light, Havey, Gourineni, Patwardhan, Sartori, and Vrbos (1994) reported about 70-85% of the forearm load at the elbow was carried by the (proximal) radius. More recently, Birkbeck, Failla, Hoshaw, Fyhrie, and Schaffler (1997) reported substantial differences in distal and proximal loads in both the radius and the ulna. The differences were eliminated after sectioning of the IOL, the primary structural passive soft tissue in the mid-forearm. Also, two recent studies clearly indicated that the IOL acts to transfer axial load from the radius to the ulna [Markolf, Lamey, Yang, Meals and Hotchkiss (1998), Pfaeffle, Fischer, Manson, Tomaino, Woo and Herndon (2000)]. All of these studies indicate that there is transfer of axial load from the radius to the ulna through the passive soft tissues of the forearm. None of these studies, however, were able to model the role of the muscles of the forearm.

It has long been postulated that bone adapts to its mechanical environment, in order to achieve an acceptable stimulus level [Roesler (1987)]. Many human [Dalén and Olsson (1974), Jones, Priest, Hayes, Tichenor and Nagel (1977), King, Brelsford and Tullos (1969), Rális, Rális, Randall, Watkins and Blake (1976), Rodriguez, Garcia-Alix, Palacios and Paniagua (1988), Rodriguez, Palacios, Garcia-Alix, Pastor and Paniagua (1988)] and animal [Goodship, Lanyon and McFie (1979), Hert, Liskova and Landa (1971), Saville and Whyte (1969), Uhthoff and Jaworski (1978)] studies in the 20^{th} century confirmed an increase in density and structural size with increased mechanical stimulus, and a decrease in density with reduced mechanical stimulus. While the specific mechanism of such adaptation remains illusive, several theories have been developed to predict adaptation to altered mechanical stimulus on a bone [Beaupré, Orr and Carter (1990b), Cowin and Hegedus (1976), Frost (1964), Hart, Davy and Heiple (1984), Huiskes, Weinans, Grootenboer, Dalstra, Fudala and Slooff (1987), Prendergast and Taylor (1992)]. Simulations based on strain-

[1] University of Kansas, Lawrence, KS, U.S.A.
[2] University of Pittsburgh, Pittsburgh, PA, U.S.A
[3] Monmouth Medical Center, Newark, NJ, U.S.A

energy density as a measure of stimulus have been successful in predicting adaptation for a broad range of problems. In addition, a computational method has been developed to estimate bone loads from bone density and geometry data [Fischer, Eckstein and Becker (1999), Fischer, Jacobs and Carter (1995), Fischer, Jacobs, Levenston, Cody and Carter (1998)]. We developed a modification of this methodology which was used in this study to evaluate the relative loads in the radius and ulna of the forearm. We hypothesized that muscle activity transfers additional load between the radius and ulna that is not accounted for in ex vivo experiments.

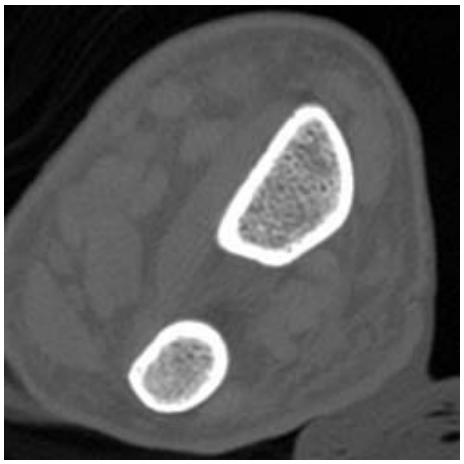

Figure 1 : CT image slice from forearm scan.

2 Methods

The approached consisted of primarily two phases. The first was the acquisition and processing of CT data from seven cadaveric specimens. Once the files were prepared, the pixel data from the radius and the ulna (from selected 2-D images) was used to estimate the relative loading of each bone.

2.1 CT Scanning and Data Processing

Seven fresh-frozen cadaveric forearms were examined in this investigation. Very limited information was available on the specimen histories. One forearm appeared osteopenic, but was not excluded from the study. Each forearm was placed in a clinical CT scanner (GE Genesis Highspeed Advantages 9800, General Electric Medical Systems, Waukesha, WI, USA) and scanned under a standard bone protocol (80 kvp, 140 ma, 1 s), at 1 mm intervals and 1 mm slice thickness. Scans were in the short axis of the forearm (cross section) and were collected sequentially in the axial direction. The image field of view was 10 cm (Fig. 1).

The raw data files were converted from DICOM format and processed using the NIH Image software. For each forearm, a single threshold value was chosen to segment the raw images and isolate the bones. Individual images of the radius and ulna were extracted as separate files (Fig. 2).

Because the CT scans were not quantitative, the density value of each pixel within an image was determined by a linear scaling, assuming the highest pixel value within the bone to have an apparent density of 1.92 g/cc and the lowest pixel value in the medullary canal to have an apparent density of 0.0 g/cc (hydrated apparent density, excluding marrow). The apparent density values at each scan level analyzed were then used to estimate the relative load in the radius and ulna.

2.2 Load Estimation Methodology

The load estimation technique is based on a strain-energy driven bone remodeling theory [Beaupré, Orr and Carter (1990a), Beaupré, Orr and Carter (1990b)]. That theory states that the bone tissue will remodel until it reaches an ideal continuum level reference stimulus (or attractor state). The attractor stimulus is formulated as a combination of stimulus intensity for a given loading condition and the number of times the load is applied over a given day (loading cycles). At equilibrium, the applied stimulus throughout the bone is equal to the attractor state stimulus, ψ_{AS}, which is mathematically formulated according to Eq. 1.

$$\psi_{AS} = \left[\sum_{i=1}^{L} n_i \overline{\sigma}_i^m\right]^{1/m} \left(\frac{\rho_c}{\rho}\right)^2 \tag{1}$$

In this equation, $\overline{\sigma}$ represents effective stress (a measure of stimulus intensity) for each load case (denoted by i), n is the number of cycles per day for each load case, m is the stress exponent which determines the relative importance of load intensity and the repetitions, L is the number of load cases, ρ_c is the maximum cortical bone apparent density (1.92 g/cc), and ρ is the local apparent bone density. The squared ratio of cortical density to apparent density is intended to scale the continuum measures of

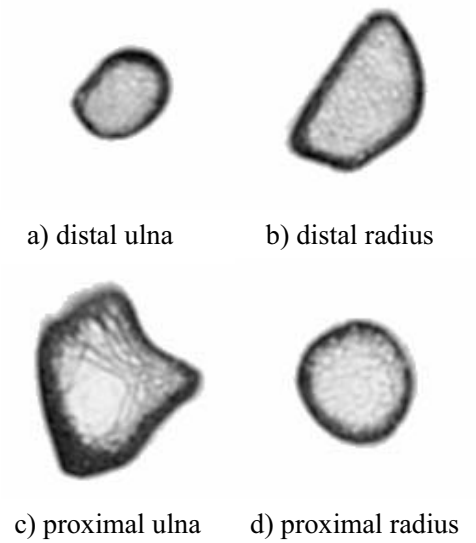

a) distal ulna b) distal radius

c) proximal ulna d) proximal radius

Figure 2 : Cross-sectional images of bones isolated from the raw CT images (inverted grayscale).

stimulus to the trabecular tissue level (at the given apparent density). The effective stress is defined according to Eq. 2.

$$\overline{\sigma}_i = \sqrt{2EU_i} \tag{2}$$

In this equation, E is the local (isotropic) elastic modulus and U is the local strain energy density for the current load case. The elastic modulus is calculated as a bilinear power function of density, and the Poisson's ratio is taken as 0.2 for $\rho \leq 1.2$ g/cc and as 0.32 for $\rho > 1.2$ g/cc [Beaupré, Orr and Carter (1990a), Orr, Beaupré, Carter and Schurman (1990)].

The load estimation theory used in this study is based on the stimulus equation and was modified from a general computational method for estimating bone loads from density distribution data [Fischer, Eckstein and Becker (1999), Fischer, Jacobs and Carter (1995), Fischer, Jacobs, Levenston, Cody and Carter (1998)]. A primary assumption of the load estimation theory is that the bone tissue has achieved remodeling equilibrium (no net apposition or resorption). Thus, all bone tissue is assumed to have a stimulus equal to the ideal reference stimulus. In the general formulation, a finite element analysis of the bone is combined with an optimization technique to determine loads that most closely produce a uniform stimulus (equal to the ideal reference) throughout the model.

Because the current analysis considers the relative load in the radius and the ulna, a modified load estimation approach was developed. For this analysis, each pixel was considered as an independent and discrete location in the bone. For a uniaxial load applied to the bone, the stress on each pixel is then equal to the applied force divided by the total cross-sectional area of the bone. For bending loads, however, the stress distribution will be non-uniform, with some points in the bone experiencing high stress, while others may experience negligible stress. Because we are only considering *overall* relative loading of the radius and ulna, the effective stress for all loads can be combined into one *overall* load magnitude measure, eliminating the sum in Eq. 1. In addition, since the number of loading cycles is the same for the radius and ulna, the number of loading cycles can be ignored (n=1), which essentially lumps the effect of loading cycles into the effective stress term (now an *overall* load magnitude measure). For the two-bone forearm system, if we assume that transverse and torsional shear stresses are negligible, only axial normal stresses will occur on each point in the bone cross section (pixel). Thus, the primary loads are assumed to be axial compression, axial tension, and bending loads. Thus, the effective stress on each element will be equal to the overall axial stress. With these simplifications, the tissue stress stimulus can be expressed as follows.

$$\psi_{AS} = \overline{\sigma}(\rho_c/\rho)^2 = [F/A_{pixel}](\rho_c/\rho)^2 \tag{3}$$

Eq. 3 can be solved directly for the force on each pixel, and summing the force contribution for all pixels in the cross section yields the total force for the bone at the proximal-distal level for the given cross section (Eq. 4).

$$F_{bone} = \left(\frac{\psi_{AS}A_{pixel}}{\rho_c^2}\right) \sum_{pixels} \rho_{pixel}^2 \tag{4}$$

Thus, for this analysis, we directly computed the axial force in each bone from the density values within each image. Forces for both bones were added to obtain total forearm force and the relative force in each bone was expressed as a percentage of the total forearm load at each proximal-distal level examined.

Relative forces (percent of forearm load for the radius and ulna) were calculated at 9 mm intervals from distal

to proximal for all seven forearm specimens. Direct measures from the image data were also evaluated for comparison with the predicted relative forces. These measures included percent of total bone cross-sectional area, average density in each bone, and percent of total cross-sectional bone mass.

3 Results

In all cases, the load estimation method predicted a consistently monotonic transfer of load from the radius to the ulna, evaluating from distal to proximal (Fig. 3-4). Only a few minor reversals in the load transfer trend were noted for the predicted relative loading. The maximum reversal of the otherwise monotonic load transfer was approximately 2% relative load.

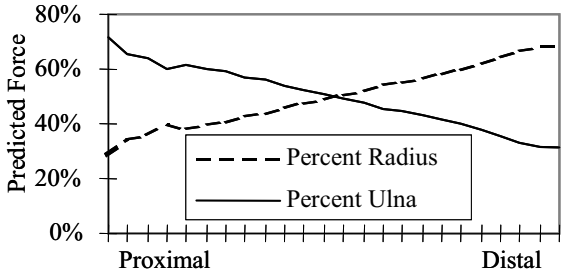

Figure 3 : Predicted percent of total forearm load for specimen 1.

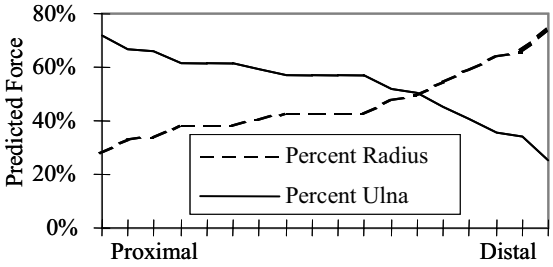

Figure 4 : Predicted percent of total forearm load for specimen 2.

Direct measures from the image data did not exhibit the consistent monotonic transfer found using the load estimation method. Percent of total bone cross-sectional area did not exhibit monotonic trends along the length of the forearm (Fig. 5). As would be expected, average density was found to be higher in the mid-forearm than proximally or distally (Fig. 6). Percent of cross-sectional bone mass was the direct measure found to best match the predicted loads (Fig. 7). Even the percent of cross-sectional bone mass, however, did not exhibit monotonic trends for all specimens (Fig. 8).

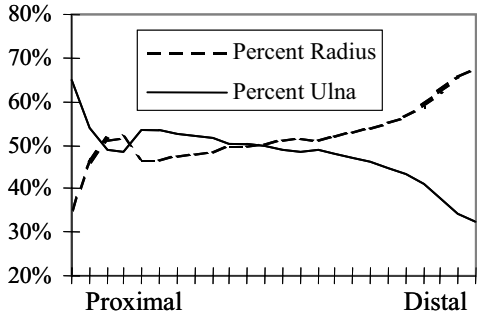

Figure 5 : Percent of total cross-sectional area for the radius and ulna (specimen 1).

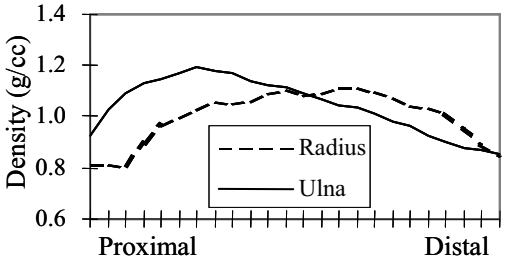

Figure 6 : Average cross-sectional apparent density for the radius and ulna (specimen 5).

Distally, the relative load in the radius averaged 69%, with a range of 64% to 75% (Tab. 1). Thus, the distal ulna loads averaged 31%, with a range of 25% to 36%. Proximally, we found an average relative load in the ulna of 71%, with a range of 62% to 81% (Tab. 2). Thus, the proximal radius loads averaged 29%, with a range of 19% to 38%.

4 Discussion

The consistent results of the relative average loads estimated from CT data of the forearm, provide a confirmation that the radius is the primary load-bearing bone at the wrist, and that the ulna is primary load-bearing bone at the elbow. These results are generally consistent with prior experimental studies [Birkbeck, Failla, Hoshaw, Fyhrie and Schaffler (1997), Markolf, Lamey, Yang, Meals and Hotchkiss (1998), Pfaeffle, Fischer, Manson, Tomaino, Herndon and Woo (1999), Pfaeffle,

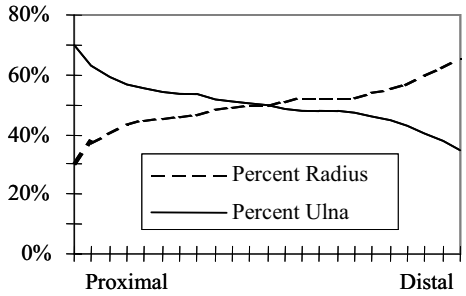

Figure 7 : Percent total cross-sectional bone mass for the radius and ulna (specimen 3).

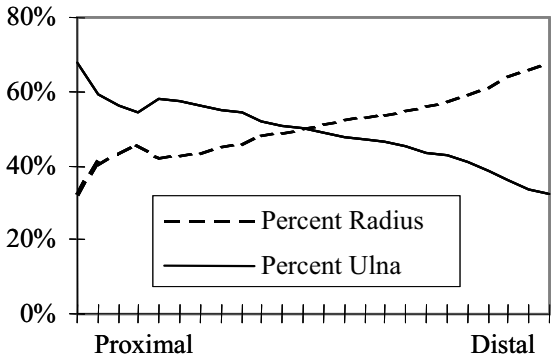

Figure 8 : Percent total cross-sectional bone mass for the radius and ulna (specimen 1).

Table 1 : Percent of Distal Forearm Load

Specimen	Radius	Ulna
1	68%	32%
2	75%	25%
3	64%	36%
4	66%	34%
5	69%	31%
6	72%	28%
7	70%	30%
Average	69%	31%
StdDev	3%	3%

Fischer, Manson, Tomaino, Woo and Herndon (2000)], but predict higher ulna loads at the elbow than most experiments [Birkbeck, Failla, Hoshaw, Fyhrie and Schaffler (1997), Markolf, Lamey, Yang, Meals and Hotchkiss (1998), Pfaeffle, Fischer, Manson, Tomaino, Herndon and Woo (1999), Pfaeffle, Fischer, Manson, Tomaino, Woo and Herndon (2000), Rabinowitz, Light, Havey, Gourineni, Patwardhan, Sartori and Vrbos (1994)].

Table 2 : Percent of Proximal Forearm Load

Specimen	Radius	Ulna
1	29%	71%
2	28%	72%
3	28%	72%
4	27%	73%
5	19%	81%
6	34%	66%
7	38%	62%
Average	29%	71%
StdDev	6%	6%

The primary passive structure capable of the predicted load transfer is the interosseous ligament (IOL) of the forearm. If this were the only load transfer mechanism, however, one would expect the loads along each bone to more closely match a step function, rather than a ramp function, as found. Certainly, muscles attached to both bones and the IOL could apply substantial loads *in vivo*. Current experimental forearm models cannot account for the forces directly generated by finger and wrist flexors and extensors, but attempt to model only external compressive forces and the compressive force the forearm muscles generate across the wrist [Birkbeck, Failla, Hoshaw, Fyhrie and Schaffler (1997), Markolf, Lamey, Yang, Meals and Hotchkiss (1998), Pfaeffle, Fischer, Manson, Tomaino, Herndon and Woo (1999), Pfaeffle, Fischer, Manson, Tomaino, Woo and Herndon (2000)]. The current data suggests that muscle forces across the wrist, across the elbow, and between the radius and ulna may have an important role in load transfer (and/or sharing) between the two bones. Muscle forces may also account for the differences between our predicted elbow forces and previously reported experimental data for elbow forces.

As with any investigation, the methodology employed in this study has limitations that must be considered. First is the assumption of remodeling equilibrium. This ideal state may never be fully achieved in vivo, though for consistent activity patterns it could practically be attained. Because of the limited data for each specimen, there is no way to definitively determine whether the bones should be considered to be in an equilibrium state. The consistency in the results, however, indicates that this assumption did not have a significant effect. The fact that this technique considers the *relative overall load-*

ing of the bones, as opposed to absolute loads for specific load cases is another limitation. While our data for proximal and distal forearm loads is very consistent with previous studies [Markolf, Lamey, Yang, Meals and Hotchkiss (1998), Palmer and Werner (1984), Pfaeffle, Fischer, Manson, Tomaino, Woo and Herndon (2000)], our data is not linked to a specific loading case. Again, however, the internal consistency of our data and consistency with other studies provides substantial confidence in the results. As others have demonstrated and discussed segmentation parameters can affect the bone geometry and, thus, the results of this study [Ho Ba Tho (2003)]. Finally, this technique neglects possible transverse and torsional shear stresses. Because the forearm consists of two bones, pure torsion on either bone is unlikely. Transverse shear (either from direct transverse loading or from torsion of the entire forearm) is likely to result in non-negligible shear for some load cases. Axial loading conditions, however, are clearly dominant in the forearm. Again, we believe the consistency of our data with studies of axial forearm compression provides a measure of validation.

While the method has some limitations noted above, we believe it has provided unique and valuable information about in vivo loads in the radius and ulna. Certainly, this initial application should be considered preliminary. Additional studies should be performed to further investigate the validity and utility of this method for estimating relative bone loads.

5 Conclusions

We conclude that there is a continuous and monotonic load transfer from the radius (carrying the majority of load distally) to the ulna (carrying the majority of load proximally). The bones themselves confirm this load transfer from their cross-sectional area and density distribution.

The muscles are the only structures (other than the IOL) with the potential for load transfer between the forearm bones. Because the load transfer was distributed along the forearm, instead of concentrated in the region of the interosseous ligament, we also conclude that muscle forces may also play an important role in load transfer. Still, we acknowledge that the IOL experiences significant loads (and acts as a major load transfer mechanism) during normal activities of daily living [Markolf, Lamey, Yang, Meals and Hotchkiss (1998), Pfaeffle, Fischer, Manson, Tomaino, Woo and Herndon (2000)].

Finally, we conclude that the density-based relative load estimation appears to be a useful tool for examining relative *in vivo* loads. The method was successful at predicting the expected forearm bone loads near the wrist and the overall load transfer between the radius and ulna.

References:

Beaupré, G. S.; Orr, T. E.; Carter, D. R. (1990a): An approach for time-dependent bone modeling and remodeling—application: a preliminary remodeling simulation. *J Orthop Res*, vol. 8, pp. 662-670.

Beaupré, G. S.; Orr, T. E.; Carter, D. R. (1990b): An approach for time-dependent bone modeling and remodeling—theoretical development. *J Orthop Res*, vol. 8, pp. 651-661.

Birkbeck, D. P.; Failla, J. M.; Hoshaw, S. J.; Fyhrie, D. P.; Schaffler, M. B. (1997): The interosseous membrane affects load distribution in the forearm. *J Hand Surg [Am]*, vol. 22, pp. 975-980.

Cowin, C.; Hegedus, D. H. (1976): Bone remodeling I: theory of adaptive elasticity. *J Elasticity*, vol. 6, pp. 313-326.

Dalén, N.; Olsson, K. E. (1974): Bone mineral content and physical activity. *Acta Orthopaedica Scandinavica*, vol. 45, pp. 170-174.

Fischer, K. J.; Eckstein, F.; Becker, C. (1999): Density-based load estimation predicts altered femoral load directions for coxa vara and coxa valga. *J Musculoskeletal Res*, vol. 3, pp. 83-92.

Fischer, K. J.; Jacobs, C. R.; Carter, D. R. (1995): Computational method for determination of bone and joint loads using bone density distributions. *J Biomechanics*, vol. 28, pp. 1127-1135.

Fischer, K. J.; Jacobs, C. R.; Levenston, M. E.; Cody, D. D.; Carter, D. R. (1998): Bone load estimation for the proximal femur using single energy quantitative CT data. *Comp Meth Biomech Biomed Engr*, vol. 1, pp. 233-245.

Frost, H. M. (1964): *The Laws of Bone Structure*, Charles C. Thomas, Springfield, Illinois.

Goodship, A. E.; Lanyon, L. E.; McFie, H. (1979): Functional adaptation of bone to increased stress. An experimental study. *J Bone Joint Surg [Am]*, vol. 61, pp. 539-546.

Hart, R. T.; Davy, D. T.; Heiple, K. G. (1984): Math-

ematical modeling and numerical solutions for functionally dependent bone remodeling. *Calcif Tissue Int*, vol. 36 Suppl 1, pp. S104-109.

Hert, J.; Liskova, M.; Landa, J. (1971): Reaction of bone to mechanical stimuli. 1. Continuous and intermittent loading of tibia in rabbit. *Folia Morphol*, vol. 19, pp. 290-300.

Ho Ba Tho, M. C. (2003): Bone and joints modeling with individualized geometric and mechanical properties derived from medical image. *CMES: Computer Modeling in Engineering & Sciences*, vol 4, no. 3&4, pp. 489-496.

Huiskes, R.; Weinans, H.; Grootenboer, H. J.; Dalstra, M.; Fudala, B.; Slooff, T. J. (1987): Adaptive bone-remodeling theory applied to prosthetic-design analysis. *J Biomechanics*, vol. 20, pp. 1135-1150.

Jones, H. H.; Priest, J. D.; Hayes, W. C.; Tichenor, C. C.; Nagel, D. A. (1977): Humeral hypertrophy in response to exercise. *J Bone Joint Surg [Am]*, vol. 59, pp. 204-208.

King, J.; Brelsford, H. J.; Tullos, H. S. (1969): Analysis of the pitching arm of the professional baseball pitcher. *Clin Orthop*, vol. 67, pp. 116-123.

Markolf, K. L.; Lamey, D.; Yang, S.; Meals, R.; Hotchkiss, R. (1998): Radioulnar load-sharing in the forearm. A study in cadavera. *J Bone Joint Surg [Am]*, vol. 80, pp. 879-888.

Orr, T. E.; Beaupré, G. A.; Carter, D. R.; Schurman, D. J. (1990): Computer predictions of bone remodeling around porous-coated implants. *J Arthroplasty*, vol. 5, pp. 191-200.

Palmer, A. K.; Werner, F. W. (1984): Biomechanics of the distal radioulnar joint. *Clin Orthop*, vol. 187, pp. 26-35.

Pfaeffle, H. J.; Fischer, K. J.; Manson, T. T.; Tomaino, M. M.; Herndon, J. H.; Woo, S. L.-Y. (1999): A new methodology to measure load transfer through the forearm using multiple universal force sensors. *J Biomechanics*, vol. 32, pp. 1331-1335.

Pfaeffle, H. J.; Fischer, K. J.; Manson, T. T.; Tomaino, M. M.; Woo, S. L.-Y.; Herndon, J. H. (2000): Role of the forearm interosseous ligament: is it more than longitudinal load transfer? *J Hand Surg [Am]*, vol. 25, pp. 683-688.

Prendergast, P.; Taylor, D. (1992): Design of intramedullary prostheses to prevent bone loss: predictions based on damage-stimulated remodelling. *J Biomed Eng*, vol. 14, pp. 499-506.

Rabinowitz, R. S.; Light, T. E.; Havey, R. M.; Gourineni, P.; Patwardhan, A. G.; Sartori, M. J.; Vrbos, L. (1994): The role of the interosseous membrane and triangular fibrocartilage complex in forearm stability. *J Hand Surg [Am]*, vol. 19, pp. 385-393.

Rális, Z. A.; Rális, H. M.; Randall, M.; Watkins, G.; Blake, P. D. (1976): Changes in shape, ossification and quality of bones in children with spina bifida. *Dev Med Child Neurol Suppl*, vol. 18, pp. 29-41.

Rodriguez, J. I.; Garcia-Alix, A.; Palacios, J.; Paniagua, R. (1988): Changes in the long bones due to fetal immobility caused by neuromuscular disease. A radiographic and histological study. *J Bone Joint Surg [Am]*, vol. 70, pp. 1052-1060.

Rodriguez, J. I.; Palacios, J.; Garcia-Alix, A.; Pastor, I.; Paniagua, R. (1988): Effects of immobilization on fetal bone development. A morphometric study in newborns with congenital neuromuscular diseases with intrauterine onset. *Calcif Tissue Int*, vol. 43, pp. 335-339.

Roesler, H. (1987): The history of some fundamental concepts in bone biomechanics. *J Biomechanics*, vol. 20, pp. 1025-1034.

Saville, P. D.; Whyte, M. P. (1969): Muscle and bone hypertrophy. Positive effect of running exercise in the rat. *Clin Orthop*, vol. 65, pp. 81-88.

Uhthoff, H. K.; Jaworski, Z. F. (1978): Bone loss in response to long-term immobilisation. *J Bone Joint Surg [Br]*, vol. 60, pp. 420-429.